Production of iron nanoparticles by laser irradiation in a simulation of lunar-like space weathering

Sho Sasaki*, Keiko Nakamura†, Yoshimi Hamabe*, Erika Kurahashi* & Takahiro Hiroi‡

** Department of Earth and Planetary Science, The University of Tokyo, Tokyo 113-0033, Japan*
† Department of Earth and Planetary Sciences, Kobe University, Kobe 657-8501, Japan
‡ Department of Geological Sciences, Brown University, Providence, Rhode Island 02912, USA

'Space weathering' is the term applied to the darkening and reddening of planetary surface materials with time, along with the changes to the depths of absorption bands in their optical spectra. It has been invoked to explain the mismatched spectra of lunar rocks and regolith, and between those of asteroids and meteorites[1–6]. The formation of nanophase iron particles on regolith grains as a result of micrometeorite impacts or irradiation by the solar wind has been proposed as the main cause of the change in the optical properties[7,8]. But laboratory simulations[9–14] have not revealed the presence of these particles, although nanosecond-pulse laser irradiation did reproduce the optical changes[12]. Here we report observations by transmission electron microscopy of olivine samples subjected to pulse laser irradiation. We find within the amorphous vapour-deposited rims of olivine grains nanophase iron particles similar to those observed in the rims of space-weathered lunar regolith grains[15,16]. Reduction by hydrogen atoms implanted by the solar wind is therefore not necessary to form the particles. Moreover, the results support the idea that ordinary chondrites came from S-type asteroids[5], and thereby provides some constraints on the surface exposure ages of those asteroids.

Space weathering was originally proposed to explain the spectral difference between lunar soils and underlying rocks, and it might also explain spectral mismatches between asteroid types and meteorite classes, especially S-type asteroids and ordinary chondrites. Lunar soil studies indicated that space weathering may be caused by the accumulation of the dark agglutinitic glass formed by melting of regolith by meteorite impacts[1]. However, the optical changes may principally be caused[7] by nanophase iron particles (about 10 nm in size) within coatings produced by recondensation of ferrous silicate vapour. Impact heating of micrometeorites and interplanetary dust particles is a process that could plausibly produce the vapour, although the sputtering and implantation of solar wind particles could also cause the surface alteration. Recently, a theoretical scattering model has shown that nanophase iron particles on grain surface rims should darken and redden the reflectance spectra of ordinary chondrites and lunar soils[8]. In fact, nanophase iron particles were found on the vapour-deposited rims of lunar soil grains[15,16]. An important consortium study on lunar soils[6] has shown that space weathering on the Moon cannot be explained solely by agglutinitic glasses: the formation of nanophase iron particles may also control the change of optical properties, especially reddening.

Previously, heating experiments have been performed to simulate space weathering. Spectral changes after the melting of meteorite samples by a fusion furnace were measured but the changes were caused by glass formation[9]. Using a pulse laser as a heating device, changes of reflectance spectra were observed[10]. However, the laser pulse duration was 0.5–1 μs, which was 1,000 times longer than the feasible timescale of micrometeorite (1–10 μm size) impacts. The laser-treated samples were molten and the resultant spectral changes should be ascribed to glass formation.

In order to simulate space weathering by high-velocity dust impact, we irradiated pellet samples of olivine and pyroxene with a pulse laser beam (1,064 nm) under a vacuum at $(1–2) \times 10^{-5}$ torr. The pulse duration was 6–8 ns, which is comparable to the timescale of dust impacts[11,12]. Laser-irradiated samples showed significant reddening: reduction of reflectance was much larger in the visible wavelength region than in the near-infrared. Reflectances of olivines are more easily changed[11] than those of pyroxenes; this result is compatible with compiled reflectance data on asteroids[13,14]. Some of the visible–near-infrared asteroid spectra can be reproduced[14] by mixing spectra of laser-irradiated olivine and pyroxene samples.

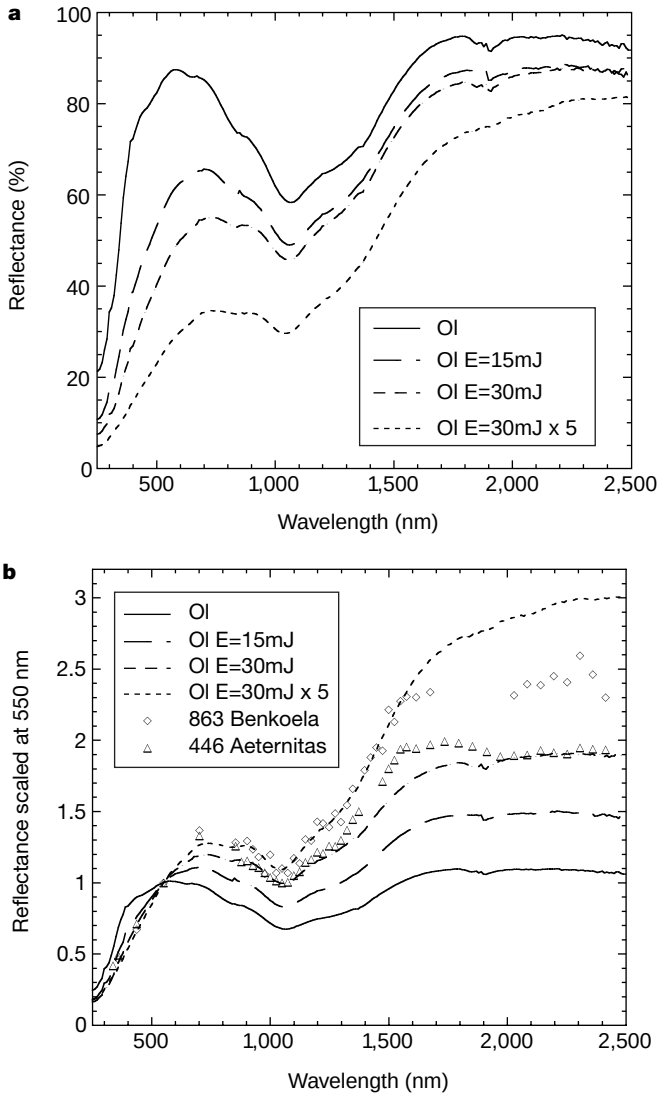

Figure 1 Bidirectional reflectance spectra of olivine pellet samples before and after pulse laser irradiation. Each 2-cm pellet is made up of grains smaller than 75 μm. The area uniformly irradiated by pulse laser has dimensions 1 cm × 1 cm, and the central millimetre-sized region of the pellet is carefully selected for measurements of bidirectional reflectance spectrum. Spectra are measured at the facility installed at the Tsukuba Space Center of the National Space Development Agency of Japan; a spectrum range between 250 and 2,500 nm is recorded at every 10 nm. **a**, Absolute spectra of olivine. **b**, Olivine spectra scaled at 550 nm. There are four spectra (non-irradiated, 15-mJ irradiation, 30-mJ irradiation, and five repetitions of 30-mJ irradiation treatment). The scaled spectra are compared with A-type asteroids 446 Aeternitas and 863 Benkoela which are considered to belong to an olivine-rich clan of S-type because of their lack of the 2-μm absorption band.

To visualize the microscopic effects causing reflectance changes, we performed repetitive pulse laser irradiations on olivine pellet samples and observed the irradiated samples using transmission electron microscopy (TEM) after obtaining reflectance measurements. We use San Carlos Olivine with 8.97 wt% FeO (Fo_{91}). Reflectance spectra of raw and laser-irradiated samples are shown in Fig. 1. In the absolute spectrum (Fig. 1a), reflectance at 500 nm decreased by 51% after 30 mJ irradiation and by as much as 67% after a five-repetition irradiation treatment of 30 mJ. Compared with the large depletion in visible reflectance, infrared reflectance decreased by only 20–30% even after five repetitions of 30-mJ irradiation. As a result, after repeated irradiations, the spectrum becomes more reddened, which is evident in the scaled spectra (Fig. 1b). The absolute depth of the 1-μm absorption band becomes shallower but the 1-μm band still remains detectable in the scaled spectrum. In Fig. 1b, spectra are compared with the observed spectra of asteroids which are considered to be olivine-rich[17]. In particular the 446 Aeternitas spectrum is close to the olivine spectra after 30-mJ irradiation. The scaled spectra of irradiated olivine are compatible with the flattening of S-asteroid spectra at wavelengths longward of 1.5 μm[18,19]. The more reddened slope of the 863 Benkoela spectrum is reproduced by that of a five-repetition 30-mJ irradiation treatment at wavelengths shorter than 1.5 μm, although repeated irradiation produced continuously red spectrum at longer wavelengths.

Several grains from each olivine pellet sample after being irradiated five times or twenty times were thin-sectioned for TEM measurement. The initial olivine San Carlos sample was also prepared for the comparable investigation. The rim regions of the irradiated olivine samples (amorphous rims of ~200-nm thickness) are developed along the grain rims. In high-resolution TEM images, nanophase particles (several up to 30 nm in size) are recognized that are widely dispersed throughout the amorphous rims (Fig. 2). These particles appear to be single- to poly-crystallines embedded within the amorphous material. Neither nanophase particles nor amorphous rims were observed on initial unirradiated olivine samples. The electron diffraction patterns from these crystallines show typical α-Fe patterns (body-centred cubic, the unit length $a_0 = 0.2874$ nm). In the high-resolution TEM images, we observe a regular 0.204-nm basal spacing which is consistent with the spacing of a crystal lattice plane (110) of α-Fe ($d_{110} = a_0/\sqrt{2} = 0.203$ nm). The energy-dispersive X-ray analyses on the regions where these nano-phase particles densely occur indicate that the beam-indent area is enriched in iron. Average atomic percentages of the amorphous materials of the rims from six different areas are: O, 59.05 (57.07); Si, 18.10 (14.08); Mg, 20.60 (25.05); and Fe, 2.25 (3.80); where the values in brackets are compositional data from the host olivine. The amorphous material is more silica-rich than the underlying olivine crystal. Moreover, as seen in Fig. 2b, doubled layers in rim structures are frequently observed. We may conclude that the amorphous silica rim with α-Fe nano-particles is produced by vapour deposition. Our observed α-Fe nanophase particles are clearly similar to those found in the rim of lunar soil grains in occurrence and size[15,16].

Our results suggest that we have succeeded in simulating a lunar-like space weathering process. We confirm a suspected link between the occurrence of nanophase iron in vapour-deposited grain rims and the spectroscopic optical effects of darkening and reddening. In space, heating by micrometeorite impacts on the regolith surface should produce the vapour, part of which would subsequently deposit on nearby grains. Through this process, nanophase crystalline iron particles should be formed and deposited. Our study shows

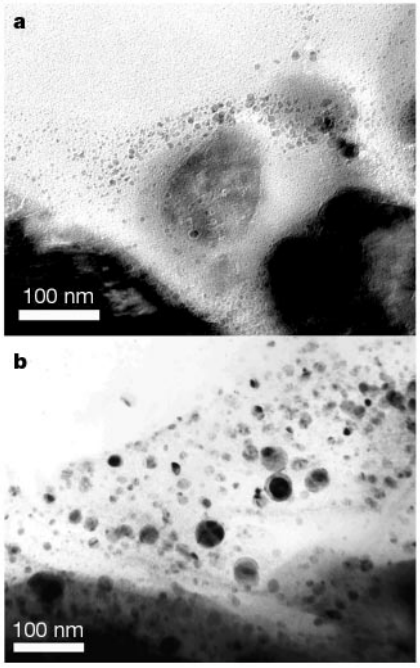

Figure 2 Nanophase iron particles in bright-field TEM images of the rim of laser-irradiated olivine grains. Selected grains from pellet samples were embedded within low viscosity epoxy (Quetol812) and thin-sectioned with ~80 nm thickness using an ultramicrotome. Imaging and electron diffraction were performed with a JEOL2010 (200 keV) TEM equipped with an energy-dispersive X-ray spectrometer at Kobe University. The electron diffraction was calibrated by using a gold-coated holey carbon film. **a**, Amorphous rim of an olivine grain from a sample irradiated 5 times at 30 mJ. There are many particles with size ranging from several nanometres to 30 nm. The boundary between host olivine crystal and amorphous rim is sharp. **b**, Doubled, possibly multiple, amorphous layers of a sample irradiated 20 times at 30 mJ. The outer rim is more widely developed than both the inner rim and the rim of the five times irradiated samples. We note that nanophase particles in the outer rim are slightly larger than those in the inner rim and polycrystallines are more ubiquitous in the outer rim.

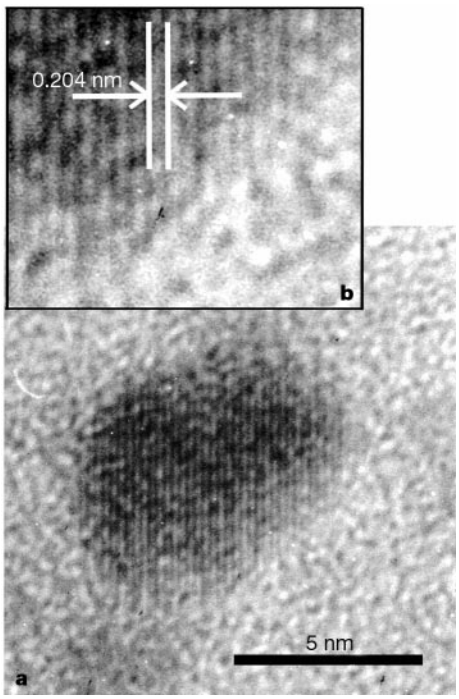

Figure 3 A nanophase particle in the rim of an olivine grain irradiated 20 times at 30 mJ. **a**, A bright-field high-resolution TEM image. The grain size is 7.7 nm. **b**, An enlarged image of **a**. The measured interlayer spacing is 0.203–0.205 nm, which is consistent with the spacing of a crystal lattice plane (110) of α-Fe ($d_{110} = 0.203$ nm).

that reduction by implanted hydrogen from solar winds is not necessary to form nanophase iron, although a previous study found formation of micrometre-scale or smaller iron particles only under hydrogen-induced reducing conditions with continuous heating[20].

Our results are compatible with recent discoveries, supporting the idea that space weathering has changed the optical properties of S-type asteroids. Although S-type asteroids are the most common in the inner part of the main asteroid belt, steep reddened reflectance spectra and derived mineralogies of S-type asteroids are different from those of ordinary chondrites, the most common meteorites[2–4]. Many small near-Earth asteroids have intermediate spectra between S-type and Q-type (ordinary-chondrite like) spectra[21]. Multispectral observation of an S-type body Ida by the Galileo spacecraft demonstrated that relatively fresh crater interiors or ejecta show colour properties similar to ordinary chondrites[5]. Furthermore, recent measurement by an X-ray spectrometer on board the NEAR-Shoemaker spacecraft showed that S-type asteroid 433 Eros has an elemental composition close to unfractionated ordinary chondrites[22]. Here we have shown that a physical process (micrometeorite impact heating) should link both with production of nanophase iron particles (Figs 2 and 3) and with spectral changes (Fig. 1) similar to those that would change ordinary chondrite spectra into S-type spectra.

Because the physical process is simulated by pulse laser heating, we can tentatively constrain the exposure ages of asteroidal regolith surfaces. The energy deposition rate in our laser experiments is 2.4×10^5 J m^{-2} at 30-mJ pulse laser irradiation[11]. In space around 1 AU, the impact rate of dust particles of around 10^{-12} g (1 μm in diameter) is a few 10^{-4} m^{-2} s^{-1} (ref. 23). Assuming a relatively high impact velocity of around 20 km s^{-1} for vaporization, the energy release rate by dust impacts is about 10^{-3} J m^{-2} yr^{-1}. When efficiencies used for heating/vaporization are the same for both laser-irradiated energy and dust-impact energy, irradiation of a 30-mJ pulse laser in our experiments corresponds to dust-impact heating over about 10^8 yr in space. Comparisons between asteroidal and laser-irradiated spectra may constrain the surface exposure age of asteroids. The energy efficiency at real micrometeorite impacts is unknown; if it is lower than that at laser irradiation as we expect, this age might be the lower limit. Our results can be applied to constrain the relative ages of optically fresh and optically mature regoliths on a single asteroid. However, care should be taken in making age comparisons between different asteroids, as the degree of space weathering should depend on the chemical composition, such as the olivine-to-pyroxene ratio, and also on the heliocentric distance, which affects the micrometeorite flux. □

Received 15 November 2000; accepted 26 January 2001.

1. Adams, J. B. & McCord, T. B. Alteration of lunar optical properties: age and composition effects. *Science* **171,** 567–571 (1971).
2. Chapman, C. R. & Salisbury, J. W. Comparison of meteorite and asteroid spectral reflectivities. *Icarus* **19,** 507–522 (1973).
3. Gaffey, M. J. & McCord, T. B. Asteroid surface materials: Mineralogical characterizations from reflectance spectra. *Space Sci. Rev.* **21,** 555–628 (1978).
4. Wetherill, G. W. & Chapman, C. R. in *Meteorites and the Early Solar System* (eds Kerridge, J. F. & Matthews, M. S.) 35–67 (Univ. Arizona Press, Tucson, 1988).
5. Chapman, C. R. S-type asteroids, ordinary chondrites, and space weathering: The evidence from Galileo's fly-bys of Gaspra and Ida. *Meteor. Planet. Sci.* **31,** 699–725 (1996).
6. Pieters, C. M. *et al.* Space weathering on airless bodies: Resolving a mystery with lunar samples. *Meteor. Planet. Sci.* **35,** 1101–1107 (2000).
7. Hapke, B., Cassidy, W. & Wells, E. Effects of vapor-phase deposition processes on the optical, chemical and magnetic properties of the lunar regolith. *Moon* **13,** 339–353 (1975).
8. Hapke, B. Space weathering in the asteroid belt. *Lunar Planet. Sci.* **31,** 1087 (2000).
9. Clark, B. E., Fanale, F. P. & Salisbury, J. W. Meteorite-asteroid spectral comparison: The effects of comminution, melting, and recrystallization. *Icarus* **97,** 288–297 (1992).
10. Moroz, L. V., Fisenko, A. V., Semjonova, L. F., Pieters, C. M. & Korotaeva, N. N. Optical effects of regolith processes on S-asteroids as simulated by laser shots on ordinary chondrite and other mafic materials. *Icarus* **122,** 366–382 (1996).
11. Yamada, M. *et al.* in *Antarctic Meteorites* Vol. 23, 173–176 (National Inst. Polar Res., Tokyo, 1998).
12. Yamada, M. *et al.* Simulation of space weathering of planet-forming materials: Nanosecond pulse laser irradiation and proton implantation on olivine and pyroxene samples. *Earth Planets Space* **51,** 1255–1265 (1999).
13. Hiroi, T. & Sasaki, S. Importance of olivine in S-asteroid space weathering. *Lunar Planet. Sci.* **30,** 1444 (1999).
14. Hiroi, T. & Sasaki, S. First successful simulation of the asteroid space weathering using reflectance spectra of pulse laser irradiated olivine and pyroxene samples—Possible compositional dependency of S-asteroid space weathering. *Meteor. Planet. Sci.* (submitted).
15. Keller, L. P. & McKay, D. S. Discovery of vapor deposits in the lunar regolith. *Science* **261,** 1305–1307 (1993).
16. Keller, L. P. & McKay, D. S. The nature and origin of rims on lunar soil grains. *Geochim. Cosmochim. Acta.* **61,** 2331–2341 (1997).
17. Gaffey, M. J. *et al.* Mineralogical variations within the S-type asteroid class. *Icarus* **106,** 573–602 (1993).
18. Clark, B. E. & Hiroi, T. S-type asteroid spectral continua: Redness and Fe, Ni metal. *Bull. Am. Astron. Soc.* **26,** 1172 (1994).
19. Clark, B. E. Spectral mixing models of S-type asteroids. *J. Geophys. Res.* **100,** 14443–14456 (1995).
20. Allen, C. C., Morris, R. V., Lauer, H. V. Jr. & McKay, D. S. Microscopic iron metal on glass and minerals—A tool for studying regolith maturity. *Icarus* **104,** 291–300 (1993).
21. Binzel, R. P., Bus, S. J., Burbine, T. H. & Sunshine, J. M. Spectral properties of near-Earth asteroids: Evidence for sources of ordinary chondrite meteorites. *Science* **273,** 946–948 (1996).
22. Trombka, J. I. *et al.* The elemental composition of asteroid 433 Eros: Results of the NEAR-Shoemaker X-ray spectrometer. *Science* **289,** 2101–2105 (2000).
23. Grün, E. *et al.* in *Origin and Evolution of Interplanetary Dust* (eds Levasseur-Regourd, A. C. & Hasegawa, H.) 21–32 (Kluwer, Dordrecht, 1991).

Acknowledgements

We thank M. Yamada for discussions and help in laser irradiation experiments, J. Owada and H. Akiyama for technical support during reflectance measurements, and H. Nagahara and K. Tomeoka for discussions and support. We thank T. Kogure for preliminary measurements by TEM and K. Akamatsu for technical advice during our TEM measurements. We also thank L. Keller for discussions on TEM analysis. We thank C. R. Chapman and B. E. Clark for their valuable comments. This work was partially supported by a Grant-in-Aid for Science Research from the Ministry of Education, Culture, Sports, Science and Technology, Japan and by a grant from the Inamori Foundation.

Correspondence and requests for materials should be addressed to S.S. (e-mail: sho@eps.s.u-tokyo.ac.jp).

Rapid magnetic reconnection in the Earth's magnetosphere mediated by whistler waves

X. H. Deng & H. Matsumoto

Radio Science Center for Space and Atmosphere, Kyoto University, Uji, Kyoto 611-0011, Japan

Magnetic reconnection has a crucial role in a variety of plasma environments[1–3] in providing a mechanism for the fast release of stored magnetic energy. During reconnection the plasma forms a 'magnetic nozzle', like the nozzle of a hose, and the rate is controlled by how fast plasma can flow out of the nozzle. But the traditional picture of reconnection has been unable to explain satisfactorily the short timescales associated with the energy release, because the flow is mediated by heavy ions with a slow resultant velocity. Recent theoretical work[4–6] has suggested that the energy release is instead mediated by electrons in waves called 'whistlers', which move much faster for a given perturbation of the magnetic field because of their smaller mass. Moreover, the whistler velocity and associated plasma velocity both increase as the 'nozzle' becomes narrower. A narrower nozzle therefore no longer reduces the total plasma flow—the outflow is independent of the size of the nozzle. Here we report observations demonstrating that reconnection in the magnetosphere is driven by whistlers, in good agreement with the theoretical predictions.

The topological change occurring during magnetic reconnection requires that the ideal magnetohydrodynamics (MHD) constraints must be broken. But the magnetosphere is essentially collisionless, like the solar corona. Traditionally it has been believed that Alfvén